

# Orbital Fulde-Ferrell-Larkin-Ovchinnikov state in 2H-NbS<sub>2</sub> flakes

Xinming Zhao,<sup>1,2,\*</sup> Guoliang Guo,<sup>2,3,\*</sup> Chengyu Yan,<sup>1,2,4,†</sup> Noah F.Q. Yuan,<sup>5</sup> Chuanwen Zhao,<sup>6</sup> Huai Guan,<sup>1,2</sup> Changshuai Lan,<sup>1,2</sup> Yihang Li,<sup>1,2</sup> Xin Liu,<sup>2,3,4,‡</sup> and Shun Wang<sup>1,2,4,§</sup>

<sup>1</sup>*Ministry of Education Key Laboratory of Fundamental Physical Quantities Measurement and Hubei Key Laboratory of Gravitation and Quantum Physics, National Precise Gravity Measurement Facility, Huazhong University of Science and Technology, Wuhan 430074, People's Republic of China*

<sup>2</sup>*School of Physics, Huazhong University of Science and Technology, Wuhan 430074, People's Republic of China*

<sup>3</sup>*Wuhan National High Magnetic Field Center, Huazhong University of Science and Technology, Wuhan 430074, People's Republic of China*

<sup>4</sup>*Institute for Quantum Science and Engineering, Huazhong University of Science and Technology, Wuhan 430074, People's Republic of China*

<sup>5</sup>*Tsung-Dao Lee Institute, Shanghai Jiao Tong University, Shanghai 201210, China and School of Physics and Astronomy, Shanghai Jiao Tong University, Shanghai 200240, China*

<sup>6</sup>*State Key Laboratory of Magnetic Resonance and Atomic and Molecular Physics, National Center for Magnetic Resonance in Wuhan, Wuhan Institute of Physics and Mathematics, Innovation Academy for Precision Measurement Science and Technology, Chinese Academy of Sciences, Wuhan 430071, Hubei, People's Republic of China*

(Dated: November 15, 2024)

Symmetry breaking in a layered superconductor with Ising spin-orbit coupling has offered an opportunity to realize unconventional superconductivity. To be more specific, orbital Fulde-Ferrell-Larkin-Ovchinnikov (FFLO) state, exhibiting layer-dependent finite-momentum pairing, may emerge in transition metal dichalcogenides materials (TMDC) in the presence of an in-plane magnetic field. Orbital FFLO state can be more robust against the magnetic field than the conventional superconducting state with zero-momentum pairing. This feature renders its potential in field-resilient superconducting functionality. Although, orbital FFLO state has been reported in NbSe<sub>2</sub> and MoS<sub>2</sub>, it is not yet clear if orbital FFLO state can be a general feature of TMDC superconductor. Here, we report the observation of orbital FFLO state in 2H-NbS<sub>2</sub> flakes and its dependence on the thickness of flake. We conclude that the relatively weak interlayer coupling is instrumental in stabilizing orbital FFLO state at higher temperature with respect to the critical temperature and lower magnetic field with respect to paramagnetic limit in NbS<sub>2</sub> in comparison to its NbSe<sub>2</sub> counterpart.

*Introduction*—Superconductivity with Cooper pairs carrying finite pairing momentum has recently stimulated opportunities to realize emerging functionality operating under conditions not feasible for superconductivity with zero-momentum pairing. For instance, finite-momentum pairing can result in superconducting diode effect exhibiting non-reciprocal supercurrent[1–4]. Although it has been known for decades that finite-momentum pairing can be routinely induced by breaking time-reversal symmetry via magnetic field, manifested as Fulde-Ferrell-Larkin-Ovchinnikov (FFLO) state[5–11], the realization of FFLO state is far from easy[10, 12, 13] owing to it requires a large magnetic field with respect to paramagnetic limit  $B_p$  and low temperature in comparison to critical temperature  $T_c$ . Fortunately, the stringent condition of activating finite-momentum pairing can be relaxed by simultaneously breaking both spatial inversion and time-reversal symmetries[4, 14–16]. This renders Rashba-superconductor[15, 17, 18] and

Ising-superconductor[4, 16, 19], with intrinsic inversion-symmetry breaking, suitable candidates for the task.

It is particularly interesting to focus on the exotic FFLO state in Ising-superconductor, referred to as orbital FFLO state[16, 20], for two reasons: First, the role of the in-plane magnetic field is dramatically different in orbital FFLO state compared to that in standard FFLO state (named as Zeeman FFLO) or FFLO state in Rashba-superconductor (labeled as Rashba FFLO). The in-plane magnetic field primarily induces Zeeman splitting in Zeeman FFLO and Rashba FFLO[5–7, 15, 17], though the impact of Zeeman effect can be reduced at most by a factor of  $\sqrt{2}$  in the case of Rashba FFLO. On the contrary, Zeeman effect of in-plane magnetic field is naturally suppressed in the presence of Ising spin-orbit coupling (SOC) with a change in the order of magnitude, instead, the in-plane magnetic field triggers a layer-dependent shift in momentum via interlayer orbital effect[4, 16, 19–21]. Second, the orbital FFLO state can potentially participate in intriguing interplay with other unconventional superconducting states in an Ising-superconductor. In an Ising-superconductor, it is known that Ising superconductivity dominates in few-layer limit[22–24], orbital FFLO state is reported in flakes with intermediate thickness[16],

\* X. Zhao and G. Guo contribute equally to the work.

† chengyu\_yan@hust.edu.cn

‡ phyliuxin@hust.edu.cn

§ shun@hust.edu.cn

whereas there is incipient evidence of Zeeman FFLO in bulk[25, 26]. However, the study of orbital FFLO is still in its infancy. It has only been recently realized in two transition metal dichalcogenides (TMDC) materials, Li-intercalated MoS<sub>2</sub>[27] and NbSe<sub>2</sub>[16] flakes. It is not yet clear if orbital FFLO can be a universal feature in Ising-superconductor.

In this work, we report the observation of orbital FFLO state in high-quality 2H-NbS<sub>2</sub> flakes. It is noticed that orbital FFLO state in NbS<sub>2</sub> qualitatively resembles that in MoS<sub>2</sub>[27] and NbSe<sub>2</sub>[16], hence suggests orbital FFLO state may be universal in TMDC or even Ising-superconductor in general. Besides, it clarifies that the formation of orbital FFLO state, whose order parameter undergoes spatial oscillation, does not rely on other spatially modulated states such as charge-density-wave (CDW) usually present in TMDC[28, 29] due to the absence of such states in NbS<sub>2</sub>. More interestingly, assembling our work with Ising superconductivity widely observed in TMDC few-layers[22–24] and Zeeman FFLO that so far only has been detected in NbS<sub>2</sub> in the entire TMDC family [25, 26], it highlights that NbS<sub>2</sub> can potentially be a model system to study the interplay between Ising superconductivity, orbital FFLO state and Zeeman FFLO state.

*Results*—Observation of orbital FFLO state puts an unprecedented requirement on sample quality to mitigate spurious effects such as surface oxidization[30] (see discussion in Supplemental Material Sec.1[31]). To ensure the high quality of 2H-NbS<sub>2</sub> flakes, we have developed a modified dry-transfer technique[32] and encapsulated the flakes with hexagonal boron nitride. As a result, the flake typically exhibits a residual resistivity ratio (RRR) exceeding 20 and a sharp superconducting transition as shown in Fig.1(a). The critical temperature  $T_c$  of flakes with thickness spanning from 45 nm down to 3.5 nm are summarized in Fig.1(b). The raw data are enclosed in Supplemental Material Sec.2[31]. It is clear that  $T_c$  drops monotonically with decreasing thickness, and can be fitted by[20, 23],

$$T_{cN} = T_{c1} + 2 \frac{J}{\alpha_0} \cos\left(\frac{\pi}{N+1}\right) \quad (1)$$

where  $T_{c1}$  denotes critical temperature of a monolayer,  $J$  quantifies interlayer Josephson coupling,  $\alpha_0$  is related to density of state of a monolayer. From the fitting, it is concluded that  $T_{c1} = 1.30$  K and  $\frac{J}{\alpha_0} = 2.25$  K, and these parameters would be later on fed to the fitting of orbital FFLO.

The signature of the orbital FFLO state is encoded in the upper critical field. The temperature dependence of the upper critical field, defined as the field value at which RH reaches 50% of resistance of normal state (details can be found in Supplemental Material Sec.3[31]), in a 19 nm flake is recorded in Fig.2(a). The raw data for flakes of different thickness are appended in Supplemental Material Sec.4[31]. The out-of-plane upper critical field  $B_{c2,\perp}$  follows 3D Ginzburg-Landau (GL) relation. On the other

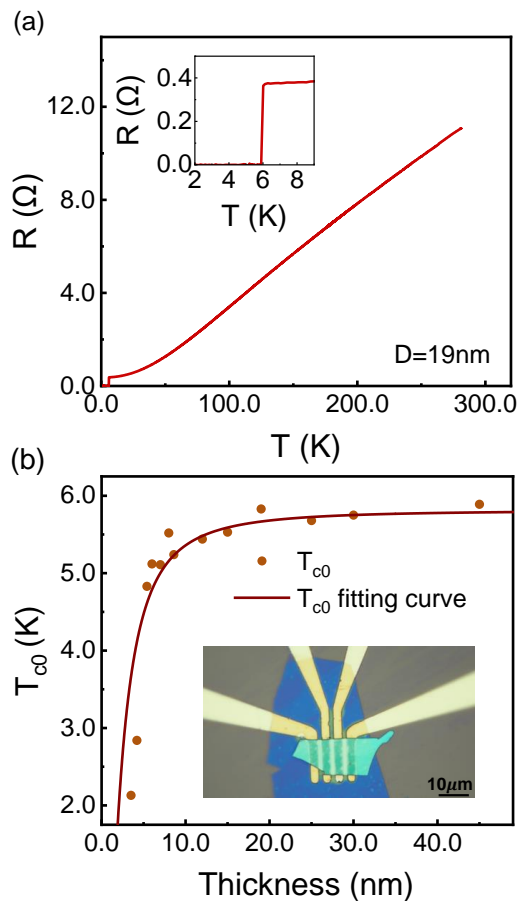


FIG. 1. (a) Typical temperature dependence of a NbS<sub>2</sub> with a thickness of 19 nm.(b) Zero-field critical temperature as a function of thickness. The experimental data is well captured by Eq.1. Inset shows the optical image of a typical device.

hand, the in-plane upper critical field  $B_{c2,\parallel}$  is initially in good agreement with 2D GL model in high-temperature regime, however, a noticeable enhancement in  $B_{c2,\parallel}$  occurs once the temperature drops below  $\sim 5.2$  K ( $0.89T_{c0}$ ), denoted as  $T^*$ . The evolution of  $B_{c2,\parallel}$  in the entire temperature range can be satisfactorily reproduced by an orbital FFLO model which treats the system effectively as weakly coupled bilayer[20, 21]. The enhancement of  $B_{c2,\parallel}$  marks the formation of orbital FFLO state with layer-dependent finite-momentum pairing below  $T^*$  whereas trivial  $B_{c2,\parallel}$  behavior arising from zero-momentum pairing dictates high-temperature regime.  $T^*$  together with the upper critical field at this temperature, marked as  $B^*$ , quantifies the tricritical point where orbital FFLO state, trivial superconductivity, and normal state merge. The overall  $B_{c2,\parallel} - T$  behaviour is qualitatively consistent with orbital FFLO state in NbSe<sub>2</sub> flakes[16] and Li-intercalated MoS<sub>2</sub>[27].

Orbital FFLO state is featured by layer-dependent stripe-like oscillation, thus highly inhomogeneous, in order parameter and breaks both translational and rotational symmetry. The direct consequence of translational

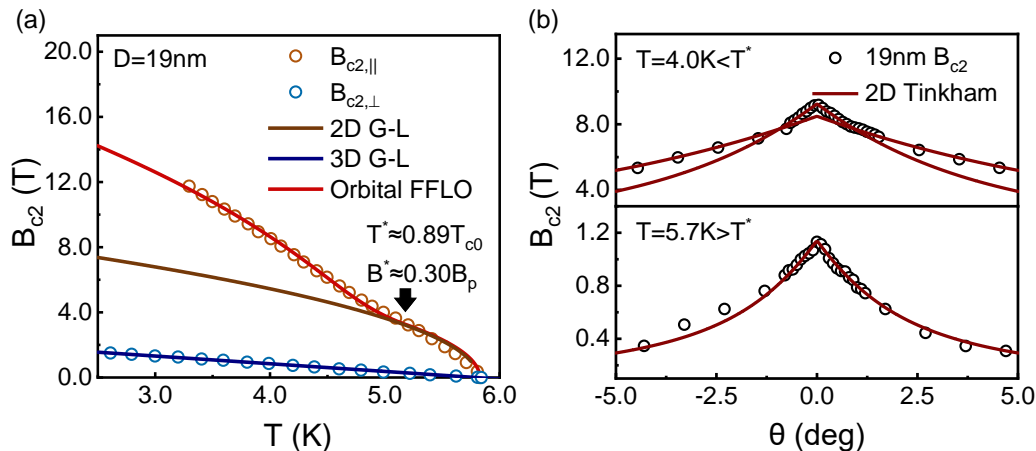


FIG. 2. (a) Evolution of upper critical field against temperature in a 19 nm flake. It is clear that in-plane upper critical field  $B_{c2,||}$  can be nicely fitted by orbital FFLO model. Detail of the model can be found in Supplemental Material Sec.1 and Sec.4[31]. (b)&(c)  $B_{c2,||}$  as a function of polar angle  $\theta$  measured at  $T = 5.7\text{K} > T^*$  and  $T = 4\text{K} < T^*$ . The in-plane orientation is defined as  $\theta = 0^\circ$ .

symmetry breaking grants its sensitivity against the out-of-plane magnetic field component, following the general trend of inhomogeneous superconducting state in layered superconductors[16, 33]. In the experiment, we validate this feature by recording  $B_{c2,||}$  with the magnetic field gradually tilting away from the in-plane direction. At  $T=5.7\text{K} > T^*$ , the polar angle dependence of  $B_{c2,||}$  takes standard 2D-Tinkham form as shown in Fig.2(b). On the other hand, the polar angle dependence has to be piecewise fitted by two 2D-Tinkham components at  $T=4\text{K} < T^*$  as highlighted in Fig.2 (c). The sharp component is responsible for  $|\theta| < 1^\circ$  and the broad one takes over at large  $\theta$ , indicating a transition from inhomogeneous order parameter to homogeneous one with increasing polar angle[16, 33]. Breaking rotational symmetry due to the formation of orbital FFLO state should install six-fold in-plane anisotropy against the magnetic field in TMDC flake[16], however, we have only managed to observe two-fold anisotropy perhaps due to the coupling between the polar and azimuthal angle of the flake (details can be found in Supplemental Material Sec.5[31]).

The observed  $B_{c2,||} - T$  relation along with polar angle dependence of  $B_{c2,||}$  can exclude other mechanisms that potentially lead to exotic  $B_{c2,||}$  behavior, such as dimensional crossover[27, 34] and dual-gap[35]. Details can be found in Supplemental Material Sec.6[31].

*Discussion*—Observation of orbital FFLO in 2H-NbS<sub>2</sub> has far-reaching impact. First, the qualitative similarity of orbital FFLO in 2H-NbS<sub>2</sub>, 2H-NbSe<sub>2</sub>[16] and Li-intercalated MoS<sub>2</sub>[27] may imply sorts of the universality of orbital FFLO state in TMDC despite the diversity in key electronic properties such as superconducting gap, interlayer coupling, spin-orbit coupling and presence of CDW or not. Second and perhaps more interesting, the Ising superconductivity is a general feature of TMDC superconductor in few-layer limit[22–24], Zeeman FFLO is reported NbS<sub>2</sub> bulk[25, 26] but not firmly established in

other TMDC materials especially NbSe<sub>2</sub>, now with the observation of orbital in 2H-NbS<sub>2</sub> flake with intermediate thickness, it suggests that there may be an intriguing evolution of Ising superconductivity  $\rightarrow$  orbital FFLO  $\rightarrow$  Zeeman FFLO with increasing flake thickness.

To shed light on the possible evolution of unconventional superconductivity in NbS<sub>2</sub>, and deviation from this routine in other TMDC materials, we summarize  $B_{c2,||}$  as a function of flake thickness in Fig.3(a).  $B_{c2,||}$  agrees well with the orbital FFLO model in thin flake of 19, 15 and 9 nm. It is helpful to mark that a recent work demonstrates that orbital FFLO state is absent in NbS<sub>2</sub> flake of 6 nm [36].  $T^*$  of the tricritical point drifts from  $0.89T_{c0}$  to  $0.87T_{c0}$  with decreasing thickness. Meanwhile,  $B^*$  sees a jump from  $0.30B_p$  (19 nm) to  $0.58B_p$  (9 nm) while  $B_p$  itself only changes by 10%. At first glance, a reduction in  $T^*$  accompanied by an enhancement in  $B^*$  can be explained by an increment in the strength of interlayer coupling[27] with decreasing thickness, however, this is against the fact that interlayer coupling weakens in thinner flake[23]. Instead, the doubling of  $B^*$  is more likely marking the onset of the interplay between orbital FFLO and Ising superconductivity, especially considering Ising SOC already has pronounced impact in 6 nm flake[36]. On the other hand,  $B_{c2,||}$  of thicker flakes changes almost linearly against temperature, however, it is noteworthy that  $B_{c2,||}$  is enhanced compared to the best linear fitting at a temperature below  $T_d=0.88T_{c0}$  and  $T_d=0.89T_{c0}$  for 25 nm and 30 nm flake while the difference in 45 nm flake is negligible. We emphasize that the deviation is always present regardless of the detail of the linear fitting, rather it has an intrinsic origin as uncovered by the polar angle dependence of  $B_{c2,||}$ . It requires dual-2D Tinkham components to capture polar angle dependence below  $T_d$  while one 2D component is sufficient for temperature above  $T_d$  in 25 nm flake as shown in Fig.3(b), qualitatively similar to the results in thinner

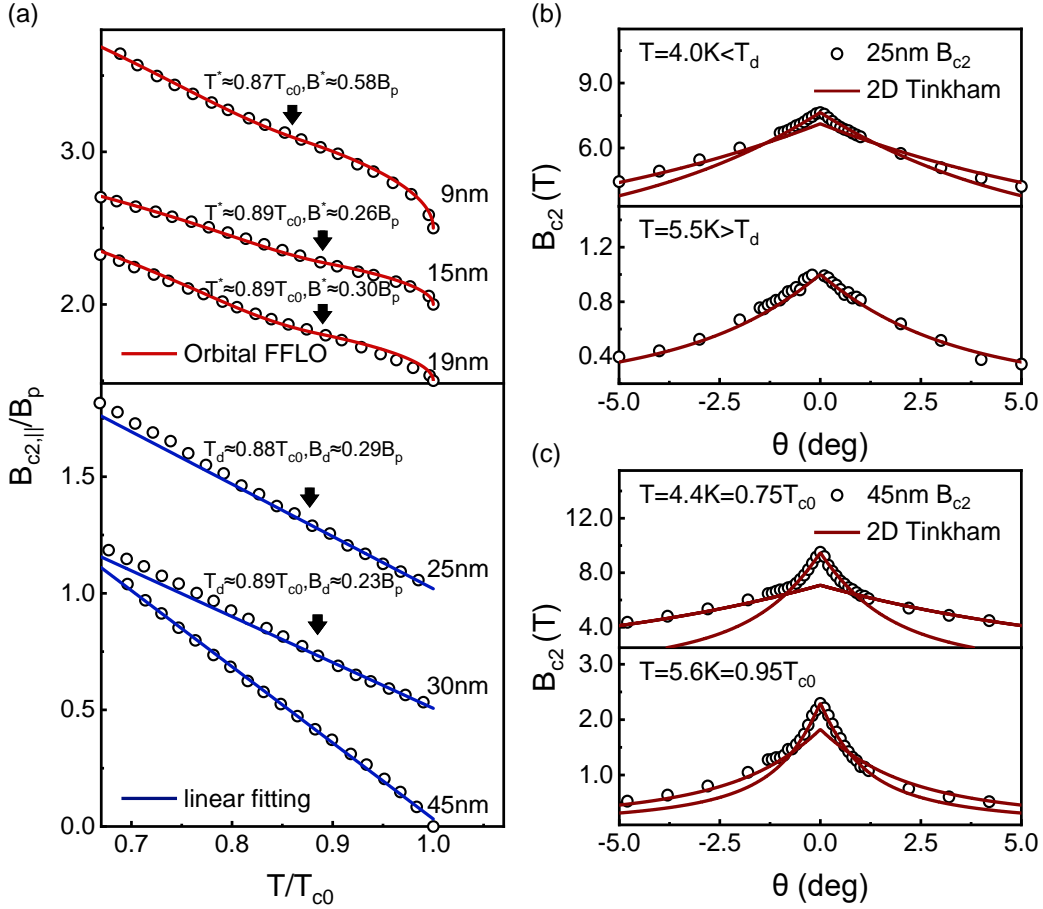


FIG. 3. (a) Thickness dependencies of  $B_{c2,||}/B_p$  as a function of  $T/T_{c0}$ . Traces are offset vertically for clarity. Enlarged version of results for each thickness can be found in Supplemental Sec.4[31]. (b)&(c) Polar angle dependence of  $B_{c2,||}$  in 25 nm and 45 nm flake, respectively.

flakes. 30 nm flake follows the same behavior, see Supplemental Material Sec.4[31]. Inspired by this, we speculate it is perhaps necessary to attribute the two linear-like segments in  $B_{c2,||}-T$  to different mechanisms: The low-temperature segment, accompanied by dual-2D Tinkham components, still arises from orbital FFLO state; The high-temperature segment does not correspond to the orbital-limit of pair breaking for 3D superconductivity, otherwise the polar angle dependence should agree with the 3D Tinkham model, instead it is a result of vortex depinning of the zero-momentum pairing superconducting state[27]. Key properties extracted from the vortex depinning effect in high temperature regime described by Klemm-Luther-Beasley theory, such as the anisotropy in the in-plane and out-of-plane coherence length and spin life time, are reasonably in agreement with that expected for  $\text{NbS}_2$ . Detailed discussion can be found in Supplemental Material Sec.4[31]. Hence,  $(T_d, B_d)$  marks the tricritical point in 25 and 30 nm flake. Likewise, the nature of the singular linear  $B_{c2,||} - T$  relation should also be carefully examined with the help of the polar angle dependence of  $B_{c2,||}$ . It is surprising that the polar angle dependence of  $B_{c2,||}$  at both  $0.95T_{c0}$  and  $0.75T_{c0}$

comprise two 2D-Tinkham components as enclosed in Fig.3(c). Therefore, the observed linear  $B_{c2,||} - T$  relation again does not correspond to orbital-limit for 3D superconductivity, and should not be compared with 3D GL model. Although we are not certain about the nature of the leading superconducting state in 45 nm flake, this state is likely to play a role in linking orbital FFLO in flakes with intermediate thickness and Zeeman FFLO in bulk.

Equipped with the thickness dependence data, it is helpful to draw a quantitative comparison between orbital FFLO states in different TMDC materials to highlight the key properties that may dominate the interplay between different unconventional superconducting state. We summarize the tricritical points of  $\text{NbS}_2$ ,  $\text{NbSe}_2$ [16] and Li-intercalated  $\text{MoS}_2$ [27] in Fig.4. It is interesting to note that  $T^*/T_{c0}$  distributes within a narrow window while  $B^*/B_p$  spans in a large range. Since  $\text{NbS}_2$  and  $\text{NbSe}_2$  are operated in the absence of intercalation whereas the formation of orbital FFLO in  $\text{MoS}_2$  depends on intercalation, it is expedient to focus on the difference between  $\text{NbS}_2$  and  $\text{NbSe}_2$  in this work while leave a more comprehensive discussion to future. Then,

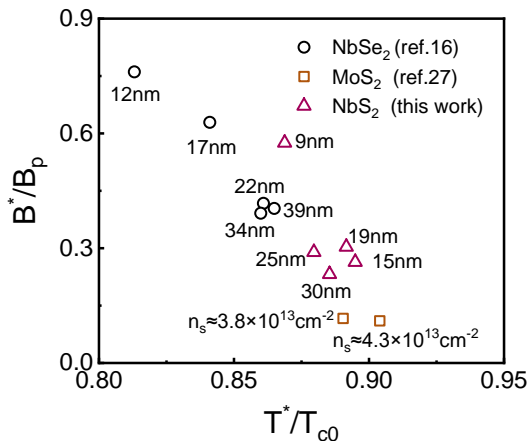


FIG. 4. Summary of tricritical points of orbital FFLO state in different TMDC materials. Data for NbSe<sub>2</sub> flakes come from ref.[16] while that for Li-intercalated MoS<sub>2</sub> bilayer are extracted from ref.[27].

it is recognized that  $B^*/B_p$  is systemically smaller and  $T^*/T_{c0}$  is consistently larger in NbS<sub>2</sub> flake compared to its NbSe<sub>2</sub> counterpart with similar thickness. Within the framework of the effective bilayer model of orbital FFLO state  $B^* \propto \sqrt{J}$  for TMDC flakes with similar flake thickness[20], with  $J$  quantifies interlayer coupling, hence the results immediately imply that interlayer coupling should be smaller in NbS<sub>2</sub> than that in NbSe<sub>2</sub>, naturally arising from the fact out-of-plane anisotropy in NbS<sub>2</sub> is considerably larger in comparison with NbSe<sub>2</sub> and will suppress interlayer coupling[26]. Interestingly,

the weak interlayer coupling in NbS<sub>2</sub> is also vital for the stabilization of Zeeman FFLO in NbS<sub>2</sub> bulk, whereas the strong interlayer coupling in NbSe<sub>2</sub> bulk prefers standard pairing[26].

*Conclusion*—We have observed orbital FFLO state with finite-momentum pairing in 2H-NbS<sub>2</sub> flakes of intermediate thickness, signified by the enhancement of in-plane upper critical field  $B_{c2,\parallel}$  and a nontrivial polar angle dependence of  $B_{c2,\parallel}$  constituted by two 2D-Tinkham components. Orbital FFLO state, zero-momentum pairing superconducting state, and normal state merge at a tricritical point ( $T^*, B^*$ ). By studying the thickness dependent of the tricritical point, we find a hint of interplay between Ising superconductivity and orbital FFLO showing as a jump in  $B^*$  accompanied by a small change in  $T^*$  with decreasing thickness in thin flake. By comparing the unconventional superconductivity in NbS<sub>2</sub> and NbSe<sub>2</sub> flake, it reveals that the relatively weak interlayer coupling in key in activating orbital FFLO in NbS<sub>2</sub> flakes at less demanding condition compared to NbSe<sub>2</sub>. Our results highlight that NbS<sub>2</sub> can be a versatile platform to explore Ising superconductivity in few-layer limit, orbital FFLO state in flakes with intermediate thickness and Zeeman FFLO in bulk-limit.

*Acknowledgments*—We acknowledge the financial support from the National Natural Science Foundation of China (Grant No. 12204184, 12074134, 12174021, 12074133) and the Innovation Program for Quantum Science and Technology (Grant No. 2021ZD0302700).

- 
- [1] Y. Hou, F. Nichele, H. Chi, A. Lodesani, Y. Wu, M. F. Ritter, D. Z. Haxell, M. Davydova, S. Ilić, O. Glezakou-Elbert, A. Varambally, F. S. Bergeret, A. Kamra, L. Fu, P. A. Lee, and J. S. Moodera, Ubiquitous Superconducting Diode Effect in Superconductor Thin Films, *Phys. Rev. Lett.* **131**, 027001 (2023).
- [2] A. Daido, Y. Ikeda, and Y. Yanase, Intrinsic Superconducting Diode Effect, *Phys. Rev. Lett.* **128**, 037001 (2022).
- [3] B. Pal, A. Chakraborty, P. K. Sivakumar, M. Davydova, A. K. Gopi, A. K. Pandeya, J. A. Krieger, Y. Zhang, M. Date, S. Ju, N. Yuan, N. B. M. Schröter, L. Fu, and S. S. P. Parkin, Josephson diode effect from Cooper pair momentum in a topological semimetal, *Nat. Phys.* **18**, 1228 (2022).
- [4] Y.-M. Xie and K. T. Law, Orbital Fulde-Ferrell Pairing State in Moiré Ising Superconductors, *Phys. Rev. Lett.* **131**, 016001 (2023).
- [5] N. F. Q. Yuan and L. Fu, Supercurrent diode effect and finite-momentum superconductors, *Proc. Natl. Acad. Sci. USA.* **119**, e2119548119 (2022).
- [6] L. P. Gor'kov, The critical supercooling field in superconductivity theory, *Sov. Phys. JETP* **10**, 593 (1960).
- [7] P. Fulde and R. A. Ferrell, Superconductivity in a Strong Spin-Exchange Field, *Phys. Rev.* **135**, A550 (1964).
- [8] S. Kasahara, Y. Sato, S. Licciardello, M. Čulo, S. Arsenijević, T. Ottenbros, T. Tominaga, J. Böker, I. Eremin, T. Shibauchi, J. Wosnitza, N. E. Hussey, and Y. Matsuda, Evidence for an Fulde-Ferrell-Larkin-Ovchinnikov State with Segmented Vortices in the BCS-BEC-Crossover Superconductor FeSe, *Phys. Rev. Lett.* **124**, 107001 (2020).
- [9] A. Bianchi, R. Movshovich, C. Capan, P. G. Pagliuso, and J. L. Sarrao, Possible Fulde-Ferrell-Larkin-Ovchinnikov Superconducting State in CeCoIn<sub>5</sub>, *Phys. Rev. Lett.* **91**, 187004 (2003).
- [10] K. W. Song and A. E. Koshelev, Quantum FFLO State in Clean Layered Superconductors, *Phys. Rev. X* **9**, 021025 (2019).
- [11] J. Clepkens and H.-Y. Kee, Finite-momentum and field-induced pairings in orbital-singlet spin-triplet superconductors, *Phys. Rev. B* **109**, 214512 (2024).
- [12] K. Kinjo, M. Manago, S. Kitagawa, Z. Q. Mao, S. Yonezawa, Y. Maeno, and K. Ishida, Superconducting spin smecticity evidencing the Fulde-Ferrell-Larkin-Ovchinnikov state in Sr<sub>2</sub>RuO<sub>4</sub>, *Science* **376**, 397 (2022).
- [13] L. W. Gruenberg and L. Gunther, Fulde-Ferrell Effect in Type-II Superconductors, *Phys. Rev. Lett.* **16**, 996 (1966).
- [14] J. Li and C. S. Ting, Single magnetic impurity in a

- spin-imbalanced superfluid Fermi gas, *Phys. Rev. B* **85**, 094520 (2012).
- [15] N. F. Q. Yuan and L. Fu, Topological metals and finite-momentum superconductors, *Proc. Natl. Acad. Sci. USA* **118**, e2019063118 (2021).
- [16] P. Wan, O. Zheliuk, N. F. Q. Yuan, X. Peng, L. Zhang, M. Liang, U. Zeitler, S. Wiedmann, N. E. Hussey, T. T. M. Palstra, and J. Ye, Orbital Fulde–Ferrell–Larkin–Ovchinnikov state in an Ising superconductor, *Nature* **619**, 46 (2023).
- [17] Z. Zheng, M. Gong, Y. Zhang, X. Zou, C. Zhang, and G. Guo, FFLO Superfluids in 2D Spin-Orbit Coupled Fermi Gases, *Sci. Rep.* **4**, 6535 (2014).
- [18] V. Barzykin and L. P. Gor'kov, Inhomogeneous Stripe Phase Revisited for Surface Superconductivity, *Phys. Rev. Lett.* **89**, 227002 (2002).
- [19] X. Zhang and F. Liu, Fulde-Ferrell-Larkin-Ovchinnikov pairing induced by a Weyl nodal line in an Ising superconductor with a high critical field, *Phys. Rev. B* **105**, 024505 (2022).
- [20] N. F. Q. Yuan, Orbital Fulde-Ferrell-Larkin-Ovchinnikov state in an Ising superconductor, *Phys. Rev. Res.* **5**, 043122 (2023).
- [21] C.-X. Liu, Unconventional Superconductivity in Bilayer Transition Metal Dichalcogenides, *Phys. Rev. Lett.* **118**, 087001 (2017).
- [22] S. C. De la Barrera, M. R. Sinko, D. P. Gopalan, N. Sivadas, K. L. Seyler, K. Watanabe, T. Taniguchi, A. W. Tsien, X. Xu, D. Xiao, and B. M. Hunt, Tuning Ising superconductivity with layer and spin-orbit coupling in two-dimensional transition-metal dichalcogenides, *Nat. Commun.* **9**, 1427 (2018).
- [23] X. Xi, Z. Wang, W. Zhao, J.-H. Park, K. T. Law, H. Berger, L. Forró, J. Shan, and K. F. Mak, Ising pairing in superconducting NbSe<sub>2</sub> atomic layers, *Nat. Phys.* **12**, 139 (2016).
- [24] J. M. Lu, O. Zheliuk, I. Leermakers, N. F. Q. Yuan, U. Zeitler, K. T. Law, and J. T. Ye, Evidence for two-dimensional Ising superconductivity in gated MoS<sub>2</sub>, *Science* **350**, 1353 (2015).
- [25] C.-w. Cho, J. Lyu, C. Y. Ng, J. J. He, K. T. Lo, D. Chareev, T. A. Abdel-Baset, M. Abdel-Hafiez, and R. Lortz, Evidence for the Fulde–Ferrell–Larkin–Ovchinnikov state in bulk NbS<sub>2</sub>, *Nat. Commun.* **12**, 3676 (2021).
- [26] C. woo Cho, C. Y. Ng, C. H. Wong, M. Abdel-Hafiez, A. N. Vasiliev, D. A. Chareev, A. G. Lebed, and R. Lortz, Competition between orbital effects, pauli limiting, and fulde–ferrell–larkin–ovchinnikov states in 2d transition metal dichalcogenide superconductors, *New J. Phys.* **24**, 083001 (2022).
- [27] D. Zhao, L. Debbeler, M. Kühne, S. Fecher, N. Gross, and J. Smet, Evidence of finite-momentum pairing in a centrosymmetric bilayer, *Nat. Phys.* **19**, 1599 (2023).
- [28] M. Leroux, M. Le Tacon, M. Calandra, L. Cario, M.-A. Méasson, P. Diener, E. Borrisenko, A. Bosak, and P. Rodière, Anharmonic suppression of charge density waves in 2H-NbS<sub>2</sub>, *Phys. Rev. B* **86**, 155125 (2012).
- [29] R. Bianco, I. Errea, L. Monacelli, M. Calandra, and F. Mauri, Quantum Enhancement of Charge Density Wave in NbS<sub>2</sub> in the Two-Dimensional Limit, *Nano Lett.* **19**, 3098 (2019).
- [30] H. Lian, Y. Wu, H. Xing, S. Wang, and Y. Liu, Effect of stoichiometry on the superconducting transition temperature in single crystalline 2H-NbS<sub>2</sub>, *Phys. C: Supercond.* **538**, 27 (2017).
- [31] See Supplemental Material for (1) The effect of sample quality on the emergence of orbital FFLO for similar thicknesses; (2) Temperature dependence for flakes with different thickness; (3) Orbital FFLO state determined with different criteria of in-plane upper critical field; (4) Raw data and fitting analysis of the upper critical field; (5) Behavior of the critical temperature as a function of azimuthal angle of the magnetic field ; (6) Exclusion of other mechanisms that can cause non-trivial  $B_{c2,\parallel} - T$  relation.
- [32] C. Zhao, X. Yi, Q. Chen, C. Yan, and S. Wang, Josephson Effect in NbS<sub>2</sub> van der Waals Junctions, *J. Phys. Chem. Lett.* **13**, 10811 (2022).
- [33] L. Bulaevskii, Inhomogeneous state and the anisotropy of the upper critical field in layered superconductors with Josephson layer interaction, *Sov. Phys. JETP* **38**, 634 (1974).
- [34] J. G. Roch, G. Froehlicher, N. Leisgang, P. Makk, K. Watanabe, T. Taniguchi, and R. J. Warburton, Spin-polarized electrons in monolayer MoS<sub>2</sub>, *Nat. Nanotechnol.* **14**, 432 (2019).
- [35] X. Bi, Z. Li, J. Huang, F. Qin, C. Zhang, Z. Xu, L. Zhou, M. Tang, C. Qiu, P. Tang, T. Ideue, T. Nojima, Y. Iwasa, and H. Yuan, Orbital-selective two-dimensional superconductivity in 2H–NbS<sub>2</sub>, *Phys. Rev. Res.* **4**, 013188 (2022).
- [36] D. Pizzirani, T. Ottenbros, M. van Rijssel, O. Zheliuk, Y. Kreminska, M. Rösner, J. F. Linnartz, A. de Visser, N. E. Hussey, J. Ye, S. Wiedmann, and M. R. van Delft, From orbital to paramagnetic pair breaking in layered superconductor 2H–NbS<sub>2</sub>, *Phys. Rev. Res.* **6**, L042006 (2024).